

Design and Optimization of Gas Sensor Testing Chamber

Fatima Ezahra Annanouch¹, Nicolas Morati¹, Virginie Martini-Laithier¹, Tomas Fiorido¹, Khalifa Aguir¹ and Marc Bendahan¹,

¹Aix Marseille Univ, Université de Toulon, CNRS, IM2NP, Marseille, France

e-mail: {fatima.annanouch, nicolas.morati, virginie.laithier, tomas.fiorido, khalifa.aguir, marc.bendahan}@im2np.fr

Gilles Bouchet², Pierre Perrier²

²Aix Marseille Univ, CNRS, IUSTI, Marseille, France

e-mail: {gilles.bouchet, pierre.perrier}@univ-amu.fr

Abstract—It is important to size and optimize the chamber in which gas sensors are tested. Indeed, the amplitude, as well as the response and recovery times are very dependent on the testing chamber. In this study, we show that by optimizing the design and reducing the volume of the testing chamber, the responses of metal oxide microsensors are highly enhanced and faster, and therefore closer to the real answers of the sensor.

Keywords—gas sensor; gas testing chamber; metal oxides; tin oxide; mathematical modeling; simulation.

I. INTRODUCTION

Metal oxide gas sensors have become one of the most active research areas, owing to their low cost and flexibility in production, simplicity of their use and their large number of detectable gases. They are employed in a wide spectrum of applications, such as environmental monitoring, domestic safety, disease detection and many more [1].

So far, many works have been reported on the enhancement of gas sensing performances, either with catalysts nanoparticles modification, or by the nanostructuring of metal oxide sensitive material [2]. However, few works have studied the influence of the gas testing system on the sensors performances. Achieving a reliable and highly sensitive sensor, with fast response and recovery times, cannot be done without an optimized gas testing chamber design. Such a design needs to be modeled and simulated in terms of chamber volume, placement of sensor and gas flow direction.

In this work we study and compare the influence of gas testing chamber design on the sensor performances, namely Cross chamber (old one) and Boat chamber (new optimized testing chamber). The paper is structured as follows. Section II describes the gas microsensor platform and the testing chamber design. Section III presents and discusses the obtained results (simulation results and experimental validation of the optimized chamber). We conclude the work in Section IV.

II. GAS SENSORS AND TESTING CHAMBERS

A. Gas sensors

The microelectromechanical systems (MEMS) based microsensor platform was patented by our laboratory and fabricated using clean room facilities and various micro-

fabrication steps including photolithography, metallization and backside etching (DRIE) of the substrate to define the membrane as the transducer [3]. This latter has a size of $400\mu\text{m} \times 400\mu\text{m}$. It carries three transducers S1, S2, S3 and two heaters (Fig. 1). The gap between the electrodes is $4\mu\text{m}$, the resistance of each heater is 100Ω and the temperature coefficient is $3 \cdot 10^{-3}/^\circ\text{C}$. An SnO_2 sensing layer (50 nm) was directly deposited over the microsensor platform, by reactive radio frequency magnetron sputtering technique [4][5].

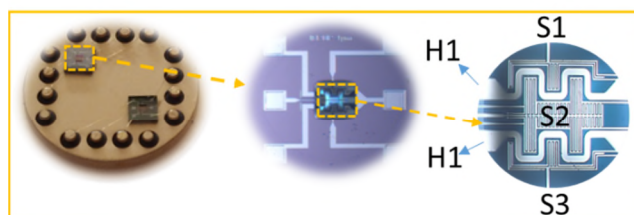


Figure 1. MEMS-based microsensor platform [3].

It is worth noting that before depositions, the microsensor platform was cleaned with acetone and then with ethanol, dried with air, and then placed inside the shadow mask.

B. Testing chambers

Gas-sensing tests were carried out in two different chambers (Fig. 2).

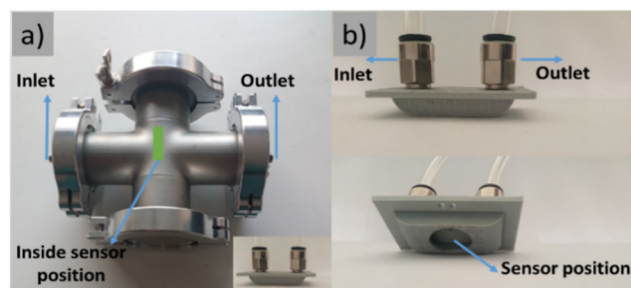


Figure 2. Photographs of: (a) cross and (b) boat chamber

The first one (Fig. 2.a) was made from stainless steel with total volume of 0.3 L and gas flow range between 0.1L/min and 1.5L/min. Besides, it has an inlet, an outlet, and the sensor optimal position is at the center, in front of the

gas flow direction. The second chamber (the new one) is illustrated by Figure 2.b. It was made from polylactic acid (PLA) with a small volume of $2.35 \cdot 10^{-3}L$ and gas flow range between 0.01 L/min and 0.5 L/min. It has a boat shape with a planar inlet and outlet. Additionally, the optimal sensor position is at the center of the boat back-side, in the same plan as the gas flow direction. In both chambers, the gas flow was maintained at 0.1 L/min, the sensor response was defined as $R=R_a/R_g$, where R_a and R_g are the sensor resistances at the stationary state in air and after 1 min of exposure to the target gas, respectively.

III. RESULTS AND DISCUSSION

A. Mathematical modelling and simulation results

The flow is modeled by a finite volume method solving the Navier-Stokes and the energy equations in the two 3D geometries, with no-slip and adiabatic boundary conditions everywhere, except on the inlet and outlet boundaries and on the sensor. Velocity fields are presented in Figure 3.

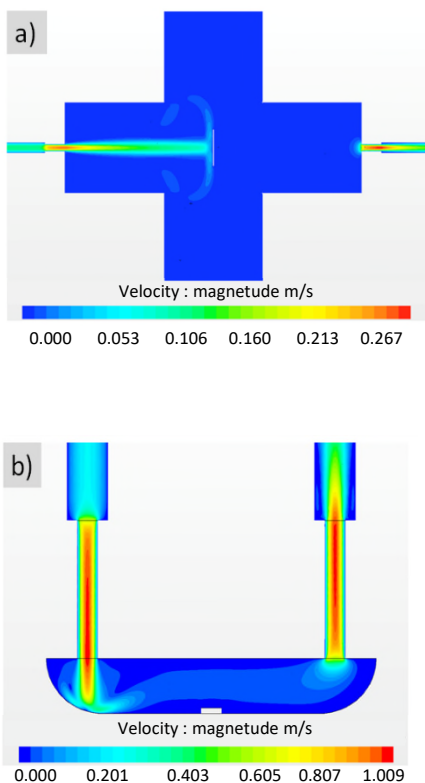


Figure 3. Velocity field of the converged flow in the Cross Chamber (a) and in the Boat chamber (b)

As we can see, in the cross chamber, at the sensor surface, the gas flow velocity is very important (0.1 m/s), which leads to the creation of many turbulences and negatively affects the sensor detection. However, in the boat chamber, it is almost zero and the gas flow direction is linear with the sensor position, which eliminates the creation of gas turbulences.

The target gas is injected at the inlet (0.1 L/min during 1 min, 50 ppm ethanol in air) and the ethanol concentration is measured on the sensor position. The gas testing transport is modeled by a convection-diffusion equation applied to a passive scalar. In Figure 4, we can observe that the gas concentration in the optimized testing chamber is very similar to the setpoint (50 ppm).

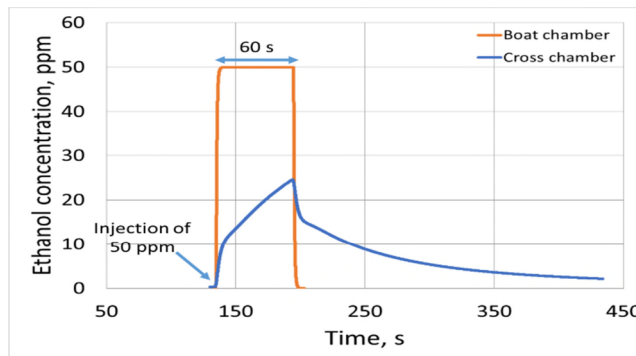


Figure 4. Ethanol concentration simulation in both chambers; injection at $t=134s$ during 1 min

In addition, the speed of the filling and emptying in boat chamber is much faster compared to the cross one. In contrast, the ethanol concentration simulated for the cross-chamber does not reach 50 ppm with a flow rate of 0.1 L/min during 60 seconds, due to the greater volume of the cross-chamber and the presence of turbulences. The simulations show that an injection lasting 10 minutes is necessary to reach 50 ppm with such flow rate; at the same time, an injection with a flow rate of 0.5 L/min for 120 seconds allows us to reach the same level of ethanol concentration (50 ppm).

These results will be experimentally validated in the next paragraph by measuring the electrical sensor response towards 50 ppm of ethanol for an exposer of 1 minute, in both chambers.

B. Validation of the optimized gas testing chamber

In order to validate the simulation results, we have exposed SnO₂ sensor (S2) to 50 ppm of ethanol, using the same measurements parameters, in both testing chambers (Fig. 5).

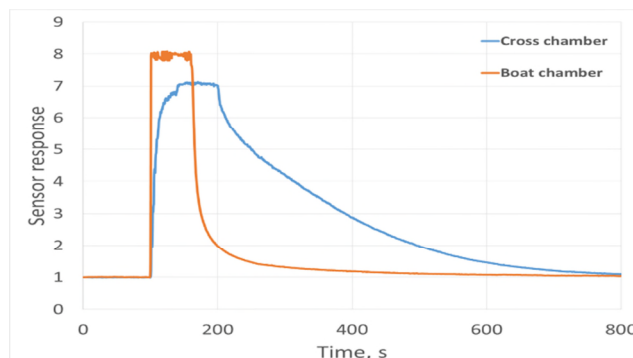


Figure 5. Experimental sensor response toward 50 ppm of ethanol in both chambers - injection during 1 min

The results show that the sensor performances are highly enhanced using the optimized chamber. For instance, the response and recovery times in the boat chamber are 4 s and 89 s, respectively. However, they are five times higher when using the cross chamber.

IV. CONCLUSION

In this study, we have highlighted the strong influence of the test chamber design with respect to the electrical response of the sensor towards ethanol. To achieve our goals, we have reduced the dimensions of the test chamber while adapting the geometry. Besides, we have eliminated dead volumes, obtained a homogeneous gas concentration, and reduced the gas flow velocity at the sensor surface. The experimental results are in agreement with the mathematical modelling and simulation results.

ACKNOWLEDGMENT

The authors would like to acknowledge NANOZ, a company specialized in gas sensors; SATT Sud-Est, "Accelerator of Technology Transfer", which is a key player

in regional economic development associated with innovation and Mr. A. Combes for his technical support.

REFERENCES

- [1] G. F. Fine, L.M. Cavanagh, A. Afonja, R. Binions, "Metal oxide semi-conductor gas sensors in environmental monitoring", *Sensors*, vol. 10, pp. 5469–5502, June 2010.
- [2] F. Annanouch et al., "Aerosol-Assisted CVD-Grown PdO Nanoparticle-Decorated Tungsten Oxide Nanoneedles Extremely Sensitive and Selective to Hydrogen", *ACS Appl. Mater. Interfaces*, vol. 8, pp. 10413–10421, April 2016.
- [3] K. Aguir, M. Bendahan, V. Laithier, "Gas sensor based on heated sensitive layer", patent N° FR 13 59494, 2013, international extension 2016.
- [4] M. Kaur et al., "RF sputtered SnO₂: NiO thin films as sub-ppm H₂S sensor operable at room temperature", *Sens. Actuators B-Chem*, vol. 242, pp. 389–403, April 2017.
- [5] G. Sberveglieri, S. Groppelli, G. Coccoli, "Radio frequency magnetron sputtering growth and characterization of indium-tin oxide (ITO) thin films for NO₂ gas sensors", *Sens. Actuators*, vol. 15, pp. 235–242, November 1988.